

## Four Regimes of Decaying Grid Turbulence in a Finite Channel

L. Skrbek, J. J. Niemela, and Russell J. Donnelly

*Cryogenic Helium Turbulence Laboratory, Department of Physics, University of Oregon, Eugene, Oregon 97403*  
(Received 8 May 2000)

Attenuation of second sound in helium II has been used to observe up to 6 orders of magnitude of decaying vorticity displaying four distinctly different regimes of decaying grid turbulence in a finite channel. A purely classical spectral model for homogeneous and isotropic turbulence describes most of the decay of helium II vorticity in the temperature range  $1.2 < T < 2$  K. The four regimes switch successively as the energy-containing and dissipative Kolmogorov length scales gradually grow during the decay, finally both being saturated by the size of the channel.

PACS numbers: 67.40.Vs, 47.27.Gs, 47.37.+q

Homogeneous and isotropic turbulence (HIT) and its decay have been the subject of extensive theoretical and experimental studies for most of the last century, which have led to a better fundamental understanding of the phenomenon of fluid turbulence in general. Numerous investigators have studied grid turbulence, regarded as nearly homogeneous and isotropic, as it decays downstream in a wind tunnel. Other investigations have involved observation of temporal decay of turbulence created by an oscillating or towed grid in a fluid under study. It is desirable to study the decay of high Reynolds number (Re) HIT possessing a well-developed inertial range. The extremely low viscosity of helium II, lowest of all known substances, allows such a goal to be reached in an apparatus of small size and under controlled laboratory conditions. We use a technique reported in [1,2], where turbulence is created by towing a grid with velocity  $V_g$  through a stationary sample of helium II and the flow is probed by second sound attenuation that depends on the quantized vortex line length per unit volume,  $L$ . A wide range of mesh Reynolds numbers ( $2 \times 10^3 \leq \text{Re}_M = V_g M \rho / \mu \leq 2 \times 10^5$ ) can be achieved easily in a small  $1 \times 1 \times 29$  cm<sup>3</sup> channel using a grid with mesh size  $M = 0.167$  cm. Here  $\mu$  is the dynamic viscosity and  $\rho$  is the density of helium II.

Helium II is a quantum fluid displaying superfluidity and, therefore, the experimental results must be interpreted with special care. In the framework of the phenomenological two-fluid model helium II is described as consisting of two independent fluids: the inviscid superfluid of density  $\rho_s$  and the normal fluid of dynamic viscosity  $\mu$  and density  $\rho_n$ , where  $\rho = \rho_s + \rho_n$ . In turbulent flow, however, the presence of quantized vortices couples the two fluids together (at least for long wavelengths), via mutual friction [3]. Based on recent theoretical and experimental investigations [3,4], in the temperature range covered in the present study, turbulent helium II flow resembles a classical flow possessing an effective kinematic viscosity  $\nu$  of order  $\mu/\rho$ . In particular, the usual HIT relationship relating turbulent energy dissipation per unit volume to the mean square vorticity applies:  $-dE/dt = \varepsilon = \nu \omega^2$ . Here the vorticity is *defined* as  $\omega(t) = \kappa L(t)$ , where  $\kappa$  is the quantum of circulation. Note that Vinen's paper [3]

is a careful study which needs to be read to understand the underlying quantum nature of this experiment. This technique allows measurements of vorticity from  $\sim 10^4$  to  $\sim 0.01$  Hz [5]. It is this unprecedented range of observed values of vorticity and flexibility in  $\text{Re}_M$  that allows detection of several distinctly different regimes of the decay and makes our system unique in the study of turbulence. Note that for most of the decay  $\omega \propto t^{-3/2}$  so that the relationship  $\varepsilon = \nu \omega^2$  implies we are observing over 8 orders of decaying turbulent energy, clearly an impossible goal for any conventional laboratory experiment (reaching such a dynamic range in a classical wind tunnel such as in [6] would require its test section to be more than 1000 km long). It has been astonishing to us that a classical model should account for such a wide range of decay. We use this method in a temperature range  $1.2 < T < 2$  K, for which  $\rho_n/\rho$  varies by more than a factor of 10. Despite this large variation in the normal fluid fraction, we observe no appreciable difference in the turbulent decay curves obtained over this wide temperature range.

An example of the decay data is shown in Fig. 1. The observed values of vorticity are evaluated from measurement of the time dependent recovery amplitude of the standing second sound resonance, initially suppressed by the presence of quantized vortices created due to motion of the grid through the channel [5]. The second sound is transmitted and detected via circular gold plated nucleopore membranes mounted flush in the wall across the channel. We therefore obtain information from a measuring volume of order  $d^3 \cong 1$  cm<sup>3</sup>. It is this natural integration that bypasses tedious statistical analysis involved in any local velocity measurements in conventional grid turbulence experiments. It provides enormous sensitivity and unprecedented dynamical range, making it very useful and complementary to classical turbulence studies.

As it takes a time  $\tau_0 \cong d/V_g$  to tow the grid through measuring volume, we use only the data obtained on time scales longer than  $\tau_0$  and  $8\tau_{LI}$ , where  $\tau_{LI}$  is the time constant of the lock-in amplifier used for detection of the amplitude of the second sound signal. The velocity of second sound exceeds that of the moving grid at least by an order of magnitude and does not restrict the time resolution

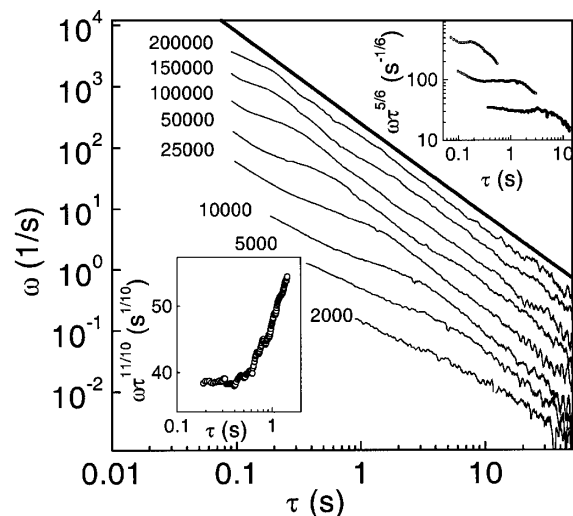


FIG. 1. The decaying helium II vorticity measured at  $T = 1.3$  K for the indicated  $Re_M$ . Each curve represents an average of three individual decays. As the decay curves tend to collapse on the universal curve, we shifted them for clarity by a factor of 2 downwards, the uppermost remaining unchanged. The early part of the vorticity decay displays a power law with exponent  $-11/10$  (see left inset, showing normalized data for  $Re_M = 10^4$ ) and later  $-5/6$  (see right inset, showing normalized data for  $Re_M = 1.5 \times 10^5$ ,  $2.5 \times 10^4$ , and  $5 \times 10^3$ ). After saturation, typically several orders of magnitude of decaying vorticity closely follow the power law with exponent  $-3/2$ , represented by the thick solid line.

of the experiment. Another time scale restriction comes from the condition how soon the grid turbulence can be considered HIT [7].

Implementing these time scale restrictions, the vorticity appears to follow  $\omega(t) \propto (t + t^*)^{-1.1} = \tau^{-1.1}$ , in agreement with the classical grid turbulence data obtained in wind tunnels, where a number of investigators found the power law  $E(t) \propto (t + t^*)^{-\alpha}$  with  $\alpha$  equal or slightly exceeding 1.2 and virtual origin time  $t^*$  around 3.5 meshes downstream [6,7]. This is the first regime of the decay (left inset in Fig. 1), widely investigated in classical wind tunnel experiments (and for most of them the only one accessible).

The decay rate then slows down and for some time the decaying vorticity displays the second regime, where it now follows a power law  $\omega(t) \propto \tau^{-5/6}$ , as evident from the right inset in Fig. 1. Later the power law changes still again and the vorticity decay follows a power law with exponent  $-3/2$ , the third regime of the decay. The switchover is clearly visible from Fig. 2 showing the compensated decay data. For the first time we report the fourth and last regime—the late exponential decay—clearly illustrated by the inset in Fig. 2.

Most of the observed decay can be predicted and described by a purely classical phenomenological spectral model of decaying HIT [2,7]. The model assumes that at early times the decaying grid turbulence displays the generally accepted form of the 3D spectrum for HIT, of a form

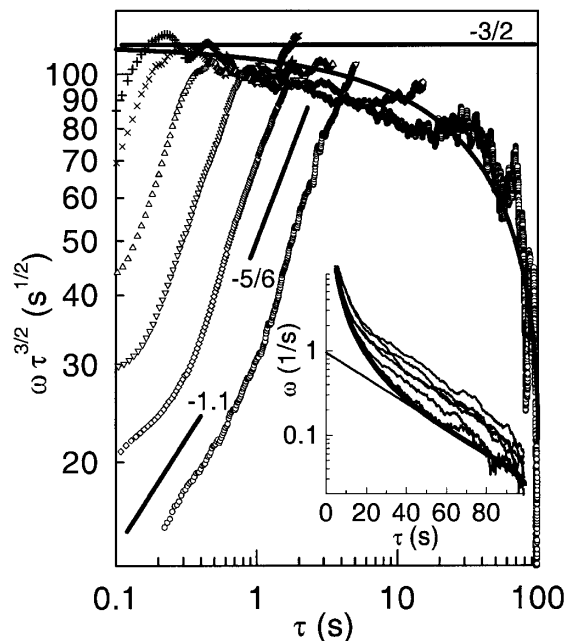


FIG. 2. The decaying vorticity multiplied by  $(t + t^*)^{3/2} = \tau^{3/2}$ , measured at  $T = 1.65$  K. The data sets from left to right correspond to  $Re_M = 2 \times 10^5$ ,  $1.5 \times 10^5$ ,  $10^5$ ,  $5 \times 10^4$ ,  $2.5 \times 10^4$ , and  $10^4$ , each being an average of three individual decays. Except for the last one, the data sets are plotted up to  $10t_{\text{sat}}$ ; the late decay for all of them is shown in the inset. The early part of the decay displays power laws with exponents  $-11/10$  and later  $-5/6$ , as indicated by straight solid lines next to the data sets. After saturation, several orders of magnitude of decaying vorticity follow expression (4), using  $C = 1.62$ ,  $\nu = 2.28 \times 10^{-4}$  cm<sup>2</sup>/s [4] and  $\gamma = 0.418$ , represented by the curved thick solid line. The influence of growing Kolmogorov length scale is indicated by the difference from the horizontal direction, representing expression (3), i.e.,  $-3/2$  power law. The inset shows the late decay of the same data sets compared with expression (4). The late decay can be characterized as exponential, of a form  $\exp(-t/t_0)$  with  $t_0 = 29$  s, represented by the straight solid line.

$$\begin{aligned}
 E(k) &= 0; & k &\leq k_d = 2\pi/d, \\
 E(k) &= Ak^m; & m &= 2 & 2\pi/d \leq k \leq k_1(t), \\
 E(k) &= C\varepsilon^{2/3}k^{-5/3}; & & & \\
 k_2(t) &\leq k \leq k_\eta^{\text{eff}} = \gamma(\varepsilon/\nu_{\text{eff}}^3)^{1/4} = 2\pi/\eta_{\text{eff}}, \\
 E(k) &= 0; & k &\geq k_\eta^{\text{eff}},
 \end{aligned} \tag{1}$$

which reflects the physical restriction that eddies larger than the size of the channel cannot exist and adopts the Kolmogorov K41 form of the inertial range, i.e., neglects intermittency. Here  $A$  is a constant with units (length <sup>$m+3$</sup> /time<sup>2</sup>). Also, the high wave number exponential tail of the spectrum is approximated by a sharp cutoff at the effective Kolmogorov length scale,  $\eta_{\text{eff}}$ , by introducing the dimensionless factor  $\gamma$  of order unity. We assume the 3D Kolmogorov constant  $C = 1.62 \pm 0.17$ , based on a number of classical experiments [8]. In the vicinity of the energy containing length scale  $l_e(t) = 2\pi/k_e(t)$ , where  $k_1(t) < k_e(t) < k_2(t)$ , the spectral energy density

displays a smooth broad maximum whose analytical form is not specified. Evaluating the total turbulent energy by integrating the 3D energy spectrum over all  $k$  leads to a differential equation for decaying turbulent energy. Applying the condition  $\varepsilon = \nu \omega^2$ , one gets a differential equation for decaying vorticity. A simplified version of the model was outlined in [2]; the full version (including intermittency corrections) has appeared elsewhere [7].

At the early decay the spectrum stays self-similar. For  $d \gg l_e \gg \eta_{\text{eff}}$ , the energy decay is predicted to follow  $E(t) \propto (t + t^*)^{-2[(m+1)/(m+3)]}$ . Comparison with both the wind tunnel [6] and helium II data [7] suggests the virtual origin position within a few mesh units downstream of the grid. This is the first regime of the decay, during which the energy containing length scale grows as  $l_e \propto (t + t^*)^{2/(m+3)}$ . Applying condition  $\varepsilon \propto \omega^2$  yields

$$\omega(t) \propto (t + t^*)^{(3m+5)/(2m+6)} = \tau^{(3m+5)/(2m+6)} \quad (2)$$

and assuming validity of the Saffman invariant ( $m = 2$ ) [9] we obtain  $\omega(t) \propto \tau^{-11/10}$ , i.e., the first regime of the decaying vorticity, as illustrated in Fig. 1. Experimentally, the power law is very sensitive to the exact value of virtual origin time. Because of the geometry of our apparatus, the parameter space for observing this first regime of the decay is rather limited, but clearly observable [7].

As the turbulence decays further and  $l_e$  grows, the lowest physically significant wave number  $k_d$  becomes closer to the broad maximum around  $2\pi/l_e$ . The low wave number part of the spectrum cannot be any longer characterized by  $Ak^m$  with  $m = 2$ , but rather by some effective power  $0 \leq m \leq 2$  that decreases as the turbulence decays. Equation (2) then shows that the decay rate slows down. As  $l_e$  approaches  $d$ ,  $m$  becomes effectively zero and we arrive at the second regime of the decay characterized by  $\omega(t) \propto \tau^{-5/6}$ . Note that these simplified power law arguments do not hold for the decay of the turbulent energy as discussed in [7].

At the saturation time  $t_{\text{sat}}$ , the vorticity reaches its saturation value  $\omega_{\text{sat}}$ . The growth of  $l_e$  is completed and subsequently  $l_e \cong d$ . Still neglecting the cutoff of the spectral energy at  $2\pi/\eta_{\text{eff}}$ , the further decay is predicted to be of the form [1,2]

$$\omega(t) = \frac{3\sqrt{3}d}{2\pi} \sqrt{\frac{C^3}{\nu_{\text{eff}}}} (t + t^{**})^{-3/2} \quad (3)$$

with the virtual origin time  $t^{**}$ . Therefore, no matter what value  $\text{Re}_M$  is (providing it is high enough to neglect viscosity corrections [7]), in the finite size box the decaying turbulence ought to reach this universal third regime of the decay.

Note that the virtual origin time  $t^{**}$  generally differs from  $t^*$  introduced above [2,7]. The simplified spectral decay model that approximates the broad energy maximum near  $l_e$  by a kink predicts  $t^{**} \cong 4t_{\text{sat}}/5$  [2], but without a detailed knowledge of the functional form of the energy spectrum near  $2\pi/l_e$  a quantitative prediction is not possible. It is plausible to assume, however, that for  $t \gg t_{\text{sat}}$

relationship (3) can be used to obtain the combination  $C^3/\nu$  [4]. From the experimental data it appears that  $t^*$  and  $t^{**}$  do not differ significantly and for our analysis of the further decay we therefore assume  $t^{**} = t^* = 3.5M/V_g$  [6].

We used individual decay curves to define  $t_{\text{sat}}$  and  $\omega_{\text{sat}}$  as an intersection point of the power laws  $\omega \propto \tau^{-5/6}$  and  $\omega \propto \tau^{-3/2}$  superimposed on the decay data. The result of this fitting procedure is summarized in Fig. 3. At all temperatures we found  $t_{\text{sat}} \propto 1/\text{Re}_M$ , in accord with the simplest variant of the spectral decay model [2]. Thus even the basic and largely simplified spectral model that approximates the broad maximum in  $E(k)$  around  $2\pi/l_e$  by a sharp kink qualitatively accounts for the change of the decay rate associated with the saturation of  $l_e$ . That  $t_{\text{sat}}$  does not depend on temperature while  $\rho_n$  changes over an order of magnitude strongly suggests that the role of quantum effects in helium II turbulence in this temperature range can be accounted for by introducing an effective kinematic viscosity [4] and justifies the applicability of a purely classical model for its decay.

So far in our discussion we neglected the role of the high wave number cutoff of the energy spectrum at  $2\pi/\eta_{\text{eff}}$ . As the turbulent energy (or vorticity) decays and the Kolmogorov length scale grows, the relative importance of this cutoff grows and a simple power law can no longer describe the decay of vorticity. It is possible to show [7] that after saturation of  $l_e$  the decaying vorticity can be more accurately described by

$$\omega(t) \cong \frac{3^3 \nu}{2^3 \gamma} \left( \frac{2\pi}{d} \right)^2 \left( \frac{t_B}{t + t^*} \right)^{3/2} \cos^3 \theta, \quad (4)$$

where

$$\begin{aligned} \cos^2(3\theta) &= \frac{t + t^*}{t_B}; \quad \text{and} \quad t_B = \frac{16C\gamma^{4/3}}{9\nu} \left( \frac{d}{2\pi} \right)^2 + t^* \\ &\cong \frac{16C\gamma^{4/3}}{9\nu} \left( \frac{d}{2\pi} \right)^2. \end{aligned} \quad (5)$$

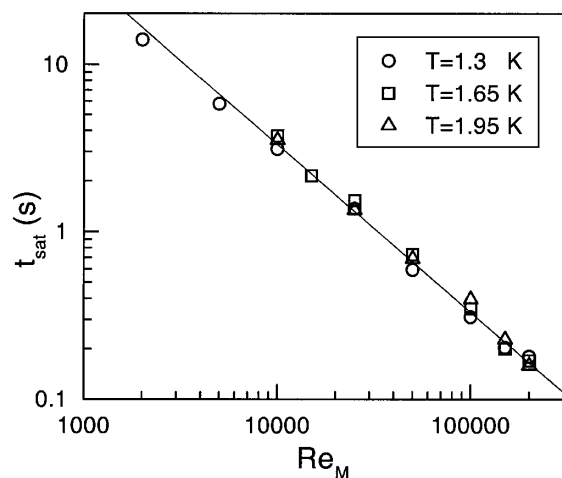


FIG. 3. Saturation time versus  $\text{Re}_M$  at different temperatures. The solid line represents  $33\,000/\text{Re}_M$ .

Naturally, for  $\gamma \rightarrow \infty$  expression (4) reduces to a simple power law (3). Formally, as the vorticity decays,  $\eta_{\text{eff}} = (2\pi\nu^{3/4}/\gamma\varepsilon^{1/4}) = 2\pi/\gamma\sqrt{\nu/\omega}$  becomes the size of the channel at a time  $t + t^* \cong 0.844t_B$ , and thus the turbulent energy becomes zero. Close to this stage the applicability of the spectral model is no longer justified. From Fig. 3 we can estimate  $t_B$  of order 100 s and using (5) we estimate  $\gamma \cong 0.4$ . This matches the value of  $\gamma$  needed to describe the viscous corrections in classical wind tunnel data [7]. Expression (4) is used for comparison with experimental data in Fig. 2. It describes the universal decay—up to 5 orders of magnitude of decaying helium II vorticity—for all starting  $\text{Re}_M$  measured at any temperature. The departure from a single power law with exponent  $-3/2$  (Fig. 2) illustrates the increasing influence of the growing Kolmogorov length scale in the decay.

Experimentally we have found a slight departure of the experimental data from the theoretical line predicted by the model towards higher values of vorticity (see Fig. 2). There might be several reasons for this behavior. First, it might occur due to extra production of vorticity by counterflow in the channel. The turbulence created by the towed grid decays and, as a result, the temperature inside the channel grows, stimulating counterflow of normal fluid and superfluid inside the channel due to the fountain effect. The faster the grid was pulled, i.e., the higher the  $\text{Re}_M$ , the more vorticity is produced by counterflow. The extra heat input could also result from friction between the grid and the channel walls. It is possible, however, that there is a deeper physical reason for this behavior originating from the quantum nature of the helium II turbulence. The quantum effects were taken into account simply by introducing the effective kinematic viscosity, somewhat larger than the kinematic viscosity based on total fluid density [4].

As the Kolmogorov scale grows, it gradually approaches  $d$  and thus  $l_e$  which is already saturated by it. Expression (4) describes the experimental data down to a surprisingly low level of vorticity, of order  $\omega \cong 0.1 \text{ s}^{-1}$ . It corresponds to the vortex line density  $L = \omega/\kappa \cong 100 \text{ cm}^{-2}$  and to the mean distance between quantized vortex lines  $l = 1/\sqrt{L} \cong 1 \text{ mm}$ . Still, the essentially classical description of the decaying vorticity holds.

With no inertial scale left there is no energy transfer towards higher wave numbers and the only possibility for further decay is exponential viscous decay. This is the fourth and last regime of decaying vorticity in a finite channel. Note that it differs from the final period of decay observed in classical wind tunnels, as these can be essentially regarded as infinitely large [2,7]. The last regime is evident from the inset of Fig. 2, where the late decay curves originating from various  $\text{Re}_M$  display an exponential decay of the form  $\omega(t) \propto \exp(-t/t_0)$ . For  $t_0 \cong 29 \text{ s}$ , the exponential decay is practically indistinguishable from the spectral model prediction. Performing systematic measurements for various  $\text{Re}_M$  at  $T = 1.3, 1.65, \text{ and } 1.9 \text{ K}$ , we obtained  $t_0 = (27 \pm 5) \text{ s}$ . Thus any possible temperature

dependence of this effect must be rather weak, within constraints of the error bars for  $t_0$ .

This last decay regime can be considered in analogy with the decay of the oscillatory motion at some particular wave number in viscous fluids, characterized by exponential decay of the energy  $E \propto E_0 \exp(-\beta t)$ , where the decay coefficient  $\beta = 2\nu k^2$  [10]. For  $k \cong 2\pi/d$  and  $\nu$  of order  $10^{-4} \text{ cm}^2/\text{s}$  it suggests a characteristic decay time close to the observed one. On the other hand, at the end of the fourth regime the vorticity has decreased to  $\cong 0.01 \text{ s}^{-1}$  implying there are only a few quantized vortex lines across the channel and applicability of any continuum theory seems questionable. Clearly the explanation of the fourth regime is a matter for further research.

To summarize, we have used superfluid helium II to investigate the decay of grid turbulence in a finite channel. We have observed up to 6 orders of magnitude of decaying helium II vorticity displaying four distinctly different regimes of decay. The form of the decay did not vary with temperature over the range  $1.2 < T < 2 \text{ K}$ , despite the fact that  $\rho_n/\rho$  changed by more than a factor of 10. The decay can be described classically, except perhaps for a slight departure from the predicted universal curve at later times. Likely reasons for this departure are the extra production of vorticity due to counterflow or a possible dependence of effective kinematic viscosity on the Reynolds number, resulting from the quantum nature of helium II turbulence. On the whole, our findings suggest a deep similarity between conventional and superfluid grid turbulence.

We thank S.R. Stalp for essential improvement of the experimental apparatus and writing the LabView code for measurements. We acknowledge stimulating discussions with G.L. Eyink, K.R. Sreenivasan, and W.F. Vinen at various stages of this work. This research was supported by NSF under Grant No. DMR-9529609.

- 
- [1] M.R. Smith, R.J. Donnelly, N. Goldenfeld, and W.F. Vinen, *Phys. Rev. Lett.* **71**, 2583 (1993).
  - [2] S.R. Stalp, L. Skrbek, and R.J. Donnelly, *Phys. Rev. Lett.* **82**, 4831 (1999).
  - [3] W.F. Vinen, *Phys. Rev. B* **61**, 1410 (2000).
  - [4] S.R. Stalp, W.F. Vinen, J.J. Niemela, and R.J. Donnelly, *Physica (Amsterdam)* **284B–288B**, 75 (2000).
  - [5] Because of the high frequency (typically 30–40 kHz) of the second sound standing wave, the frequency dependence of the mutual friction coefficient was taken into account. See C.F. Barenghi, R.J. Donnelly, and W.F. Vinen, *J. Low Temp. Phys.* **52**, 189 (1983).
  - [6] G. Comte-Bellot and S. Corrsin, *J. Fluid Mech.* **25**, 657 (1966); **48**, 273 (1971).
  - [7] L. Skrbek and S.R. Stalp, *Phys. Fluids* **12**, 1997 (2000).
  - [8] K.R. Sreenivasan, *Phys. Fluids* **7**, 2778 (1995).
  - [9] P.G. Saffman, *J. Fluid Mech.* **27**, 581 (1967); *Phys. Fluids* **10**, 1349 (1967).
  - [10] See, e.g., L.D. Landau and E.M. Lifshitz, *Hydrodynamics* (Pergamon Press, New York, 1987), 2nd ed.